2010 American Control Conference
Marriott Waterfront, Baltimore, MD, USA
June 30-July 02, 2010

Preventing transition to turbulence using streamwise traveling waves: direct numerical simulations

Binh K. Lieu, Rashad Moarref, and Mihailo R. Jovanović

Abstract— **We use direct numerical simulations of the nonlinear Navier-Stokes (NS) equations to examine the effectiveness of streamwise traveling waves for controlling the onset of turbulence in a channel flow. We highlight the effect of a base flow induced by the streamwise traveling waves on the dynamics of velocity fluctuations and on the net efficiency of control. It is shown that properly designed downstream traveling waves are capable of reducing the fluctuations' kinetic energy and maintaining the laminar flow. In contrast, our results demonstrate that upstream traveling waves promote turbulence even when the uncontrolled flow stays laminar. Our numerical simulations elucidate the predictive power of the theoretical framework developed in a companion paper [1] and suggest that the linearized NS equations with uncertainty serve as an effective control-oriented model for preventing transition.**

Index Terms— **Flow control; transition to turbulence; Navier-Stokes equations; direct numerical simulations; energy amplification; skin-friction drag coefficient.**

I. Introduction

Significant attention has recently been paid to the problems of drag reduction and turbulence suppression in transitional and turbulent channel flows using sensorless control strategies. In this setup control action is formed without measurement of the relevant flow quantities and disturbances, thereby circumventing estimation of velocity fluctuations based on noisy surface measurements (observer design in high-Reynolds-number flows is a challenging problem). In [2], it was shown by direct numerical simulations (DNS) that surface actuation in the form of an upstream traveling wave (UTW) can sustain sub-laminar skin-friction drag.

Currently available sensorless flow control strategies are designed using extensive numerical and experimental studies. For example, an extensive number of simulations on turbulent drag reduction by means of spanwise wall oscillation was conducted in [3] where 37 cases of different control parameters were considered. Instead of an extensive numerical study, this paper builds directly on the theoretical findings of a companion paper [1] where system-theoretic approach was used to show that downstream traveling waves (DTWs) are capable of weakening the sensitivity to background disturbances of the most energetic structures in a flow with no control. The effectiveness of DTWs and UTWs in preventing or enhancing transition is examined in this work.

B. K. Lieu, R. Moarref, and M. R. Jovanović are with the Department of Electrical and Computer Engineering, University of Minnesota, Minneapolis, MN 55455, USA (e-mails: lieux006@umn.edu, rashad@umn.edu, mihailo@umn.edu).

Financial support from the National Science Foundation under CAREER Award CMMI-06-44793 is gratefully acknowledged.

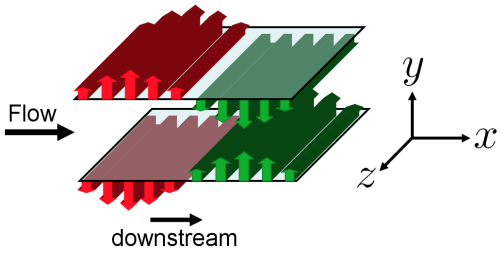

Fig. 1. A channel flow with blowing and suction along the walls.

We use high-fidelity simulations to demonstrate that the DTWs with parameters selected in [1] can prevent transition and achieve positive net efficiency relative to the uncontrolled flow that becomes turbulent. On the contrary, the UTWs induce turbulence even when the uncontrolled flow stays laminar. In spite of promoting turbulence, the UTWs with large amplitudes can provide sub-laminar drag coefficient. However, we show that this comes at the expense of poor net power balance in flows driven by fixed pressure gradient. Our numerical simulations elucidate the predictive power of the theoretical framework developed in [1] and suggest that the linearized NS equations with uncertainty represent an effective control-oriented model for maintaining the laminar flow.

Our presentation is organized as follows: in § II, we present the governing equations, describe the numerical method used in our simulations, and outline the influence of base flow on the net cost of control. The effect of traveling waves on evolution of three-dimensional (3D) fluctuations around base flow is analyzed in § III; we further highlight how dynamics of velocity fluctuations affect skin-friction drag coefficient and net cost of control. A brief summary of the main results is provided in § IV.

II. Problem formulation and numerical method

A. Governing equations

We consider an incompressible flow of a viscous Newtonian fluid in a straight 3D channel; see Fig. 1 for geometry. The spatial coordinates (x, y, z) are scaled with the channel half height, δ, and they denote the streamwise, wall-normal, and spanwise directions, respectively; the velocities are scaled with the centerline velocity of the laminar parabolic profile, U_c; the pressure is scaled with ρU_c^2, where ρ denotes the fluid density; and the time is scaled with the convective time scale, δ/U_c. The flow is driven by a streamwise pressure gradient and it satisfies the non-dimensional NS and

continuity equations

$$\mathbf{u}_t = -(\mathbf{u}\cdot\boldsymbol{\nabla})\,\mathbf{u} - \boldsymbol{\nabla}P + (1/R_c)\Delta\mathbf{u}, \quad 0 = \boldsymbol{\nabla}\cdot\mathbf{u}. \quad (1)$$

Here, R_c denotes the Reynolds number, $R_c = U_c\delta/\nu$, ν is the kinematic viscosity, $\mathbf{u}$ is the velocity vector, P is the pressure, $\boldsymbol{\nabla}$ is the gradient, and Δ is the Laplacian, $\Delta = \boldsymbol{\nabla}\cdot\boldsymbol{\nabla}$.

In addition to the constant pressure gradient, $P_x = -2/R_c$, let the flow be subject to a zero-net-mass-flux surface blowing and suction in the form of a streamwise traveling wave. The base velocity, $\mathbf{u}_b = (U, V, W = 0)$, represents the steady-state solution to (1) in the presence of the following boundary conditions

$$\begin{array}{c} V(y = \pm 1) = \mp 2\,\alpha\,\cos\left(\omega_x(x - c\,t)\right), \\ U(\pm 1) = V_y(\pm 1) = W(\pm 1) = 0, \end{array} \quad (2)$$

where ω_x, c, and α denote frequency, speed, and amplitude of the traveling wave. Positive values of c define a DTW, while negative values of c define a UTW. In the presence of velocity fluctuations, $\mathbf{u}$ represents the sum of base velocity, $\mathbf{u}_b$, and velocity fluctuations, $\mathbf{v} = (u, v, w)$, where u, v, and w denote the fluctuations in the streamwise, wall-normal, and spanwise directions, respectively.

B. Numerical method

The traveling waves that are considered theoretically in [1] are tested in DNS of a 3D transitional channel flow. All simulations performed in this work use the code developed in [4]. A multi-step semi-implicit Adams-Bashforth/Backward-Differentiation (AB/BDE) scheme described in [5] is used for time discretization. The AB/BDE treats the linear terms implicitly and the nonlinear terms explicitly. A spectral method [6] is used for the spatial derivatives with Chebyshev polynomial expansion in the wall-normal direction and Fourier series expansion in the streamwise and spanwise directions. Aliasing errors from the evaluation of the nonlinear terms are removed by the 3/2-rule when the horizontal FFTs are computed. We modified the code to account for the boundary conditions (2).

The nonlinear NS equations are integrated in time with the objective of computing the fluctuations' kinetic energy and the skin-friction drag coefficient, § III. The velocity field is first initialized with the laminar parabolic profile in the absence of 3D fluctuations, § II-C; this yields the 2D base flow which is induced by the fixed pressure gradient, $P_x = -2/R_c$, and the boundary conditions (2). In simulations of the full 3D flows (cf. § III), an initial 3D perturbation is superimposed to the base velocity, $\mathbf{u}_b$. As the initial perturbation, we consider a random velocity field which has the ability to trigger turbulence by exciting all the relevant Fourier and Chebyshev modes [4]. This divergence-free initial condition is composed of random spectral coefficients that decay exponentially and satisfy homogenous Dirichlet boundary conditions at the walls.

A fixed pressure gradient is enforced in all simulations which are initiated at $R_c = 2000$. We consider a streamwise box length, $L_x = 4\pi/\omega_x$, for all controlled flow simulations. This box length captures the streamwise modes $k_x = \{0, \pm\omega_x/2, \pm\omega_x, \pm 3\omega_x/2, \ldots\}$; relative to [1], these modes correspond to the union of the fundamental ($k_x = \{0, \pm\omega_x, \pm 2\,\omega_x, \ldots\}$) and subharmonic ($k_x = \{\pm\omega_x/2, \pm 3\omega_x/2, \ldots\}$) modes. In our presentation, in addition to the uncontrolled flow, we consider two DTWs with ($c = 5$, $\omega_x = 2$, $\alpha = \{0.035, 0.050\}$), and three UTWs with ($c = -2$, $\omega_x = 0.5$, $\alpha = \{0.015, 0.050, 0.125\}$). The number of spatial grid points in x, y, and z directions used in the uncontrolled and DTW flows are $N_x = 50$, $N_y = 65$, and $N_z = 50$, respectively; for the UTWs, we use $N_x = 200$, $N_y = 65$, and $N_z = 50$. The total integration time is $t_{tot} = 1000\,\delta/U_c$. We have verified our simulations by making sure that the changes in results are negligible by increasing the number of wall-normal grid points to $N_y = 97$; we have also established agreement of our results for UTWs with those of [2].

C. Base velocity and nominal net efficiency

The base velocity, $\mathbf{u}_b = (U(x, y, t), V(x, y, t), 0)$, is computed using DNS of a 2D channel flow with $R_c = 2000$ in the presence of streamwise traveling wave boundary control (2). The nominal bulk flux is determined by $U_{B,N} = 0.5\int_{-1}^{1}\overline{U}(y)\,\mathrm{d}y$, where overline denotes the average over horizontal directions. For the fixed pressure gradient, $P_x = -2/R_c$, the nominal skin-friction drag coefficient is inversely proportional to square of the nominal bulk, i.e., $C_{f,N} = -2\,P_x/U_{B,N}^2$ (cf. Table I). As shown in [7], compared to the uncontrolled laminar flow, the nominal flux is decreased (increased) by DTWs (UTWs); this results in larger (smaller) nominal drag coefficients, respectively.

The above results suggest that upstream traveling waves can exhibit increased flux compared to the uncontrolled flow. For the fixed pressure gradient, this results in production of a driving power

$$\Pi_{prod} = -P_x\,(U_{B,c} - U_{B,u})\,(2S),$$

where $U_{B,c}$ and $U_{B,u}$ denote the bulks of the controlled and uncontrolled flows, respectively, and $S = L_xL_z$ is the area of the wall. The normalized produced power $\%\Pi_{prod}$ is expressed as a percentage of the power spent to drive the uncontrolled flow, $\Pi_u = -P_x\,U_{B,u}\,(2S)$,

$$\%\Pi_{prod} = 100\,(U_{B,c} - U_{B,u})\,/U_{B,u}.$$

On the other hand, the input power required for maintaining the traveling waves is obtained from [8]

$$\Pi_{req} = \left(\overline{VP}\big|_{y=-1} - \overline{VP}\big|_{y=1}\right) S,$$

and the normalized required power $\%\Pi_{req}$ is expressed as

$$\%\Pi_{req} = 100\,\frac{\overline{VP}\big|_{y=-1} - \overline{VP}\big|_{y=1}}{-2\,P_x\,U_{B,u}}.$$

In order to assess the efficacy of traveling waves for controlling transitional flows, the control net power is defined as the

Case	c	ω_x	α	$U_{B,N}$	$10^3\, C_{f,N}$	$\%\Pi_{prod}$	$\%\Pi_{req}$	$\%\Pi_{net}$
0	–	–	–	0.6667	4.5000	0	0	0
1	5	2	0.035	0.6428	4.8404	−3.58	16.64	−20.22
2	5	2	0.050	0.6215	5.1778	−6.77	31.74	−38.51
3	−2	0.5	0.015	0.6703	4.4513	2.70	5.46	−2.76
4	−2	0.5	0.050	0.7791	3.2949	16.86	37.69	−20.83
5	−2	0.5	0.125	1.0133	1.9478	51.99	145.05	−93.06

TABLE I

NOMINAL RESULTS IN CHANNEL FLOW WITH $R_c = 2000$. THE NOMINAL FLUX, $U_{B,N}$, AND SKIN-FRICTION DRAG COEFFICIENT, $C_{f,N}$, ARE COMPUTED IN THE 2D SIMULATIONS OF THE BASE FLOW DESCRIBED IN § II-C. THE PRODUCED POWER, $\%\Pi_{prod}$, REQUIRED POWER, $\%\Pi_{req}$, AND NET POWER, $\%\Pi_{net}$, ARE NORMALIZED BY THE POWER REQUIRED TO DRIVE THE UNCONTROLLED FLOW. THE PRODUCED AND NET POWERS ARE COMPUTED WITH RESPECT TO THE UNCONTROLLED LAMINAR FLOW.

difference between the produced and required powers [3]

$$\%\Pi_{net} \;=\; \%\Pi_{prod} \,-\, \%\Pi_{req},$$

where $\%\Pi_{net}$ signifies how much net power is gained (positive $\%\Pi_{net}$) or lost (negative $\%\Pi_{net}$) in the controlled flow as a percentage of the power spent to drive the flow with no control.

The nominal efficiency of the selected streamwise traveling waves in 2D flows, i.e. in the absence of velocity fluctuations, is shown in Table I. Note that the nominal net power is negative for all controlled simulations. This is in agreement with a recent study of [7] where it was shown that the net power required to drive a flow with transpiration-based control is always larger than in the (standard) pressure gradient type of actuation.

III. CONTROL OF TRANSITION BY TRAVELING WAVES

It was shown in [1] that a positive net efficiency can be achieved in a situation where the uncontrolled flow becomes turbulent but the controlled flow stays laminar. Whether the controlled flow can remain laminar depends on the dynamics of velocity fluctuations around the modified base flow. In this section, we study the influence of velocity fluctuations on the control net efficiency in flows subject to streamwise traveling waves. This problem is addressed by simulating full 3D channel flows in the presence of initial fluctuations which are superimposed on the base velocity. Depending on the kinetic energy of the initial condition, we distinguish two cases: (i) both the uncontrolled and properly designed controlled flows remain laminar (*small* initial energy); and (ii) the uncontrolled flow becomes turbulent, while the controlled flow stays laminar for the appropriate choice of traveling wave parameters (*moderate* initial energy). Our simulations indicate, however, that *poorly* designed traveling waves can introduce turbulence even for initial velocity fluctuations for which the uncontrolled flow stays laminar. It was demonstrated in [1] that properly designed DTWs are capable of significantly weakening the intensity of velocity fluctuations which makes them well-suited for preventing transition; on the other hand, compared to the uncontrolled flow, the velocity fluctuations around the UTWs at best exhibit similar sensitivity to background disturbances.

The 3D simulations, which are summarized in Table II, confirm and complement the theoretical predictions in [1] at two levels. At the level of transition control, we illustrate in § III-A that the UTWs increase the intensity of velocity fluctuations and promote transition even for initial perturbations for which the uncontrolled flow stays laminar. In contrast, the DTWs can prevent transition even in the presence of initial conditions with moderate energy (cf. § III-B). At the level of net power efficiency, it is first shown in § III-A that the net power is negative when the uncontrolled flow stays laminar. However, for the uncontrolled flow that becomes turbulent, we demonstrate that the DTWs that remain laminar can result in a positive net efficiency. Our simulations in § III-B reveal that although UTWs become turbulent, a positive net efficiency can be achieved for small enough wave amplitudes. For the initial conditions with moderate energy, we further point out that the achievable positive net efficiency for UTWs is much smaller than for the DTWs that sustain the laminar flow (cf. § III-B).

A. Small initial energy

We first consider the initial fluctuations with small kinetic energy, $E(0) = 2.25\times10^{-6}$, which cannot trigger turbulence in the uncontrolled flow. Our simulations show that the DTWs with parameters suggested in [1] improve transient response of the velocity fluctuations; on the contrary, the UTWs with parameters considered in [2] lead to deterioration of the transient response and, consequently, enhance turbulence production. Since the uncontrolled flow stays laminar, both DTWs and UTWs lead to the negative net efficiency.

The energy of velocity fluctuations is given by

$$E(t) \;=\; \frac{1}{\Omega}\int_{\Omega}(u^2+v^2+w^2)\,\mathrm{d}\Omega,$$

where $\Omega = 2S$ is the volume of the computational box. Fig. 2 shows the fluctuations' kinetic energy as a function of time for the uncontrolled and controlled flows. As evident

Initial Energy	Case	c	ω_x	α	$10^3\, C_f$	$\%\Pi_{prod}$	$\%\Pi_{req}$	$\%\Pi_{net}$
Small	0	–	–	–	4.5002	0	0	0
	2	5	2	0.050	5.1778	−6.77	31.77	−38.54
	3	−2	0.5	0.015	4.3204	−1.54	5.14	−3.60
	4	−2	0.5	0.050	5.9426	−16.52	23.22	−39.74
	5	−2	0.5	0.125	3.6853	12.20	108.41	−96.21
Moderate	0	–	–	–	10.3000	0	0	0
	1	5	2	0.035	4.9244	52.07	26.44	25.63
	2	5	2	0.050	5.2273	47.35	50.40	−3.05
	3	−2	0.5	0.015	8.7866	11.36	4.53	6.83
	4	−2	0.5	0.050	6.7406	31.15	41.96	−10.81
	5	−2	0.5	0.125	3.9264	77.03	155.80	−78.77

TABLE II

RESULTS OF 3D SIMULATIONS IN CHANNEL FLOW WITH $R_c = 2000$. THE VALUES OF C_f, $\%\Pi_{prod}$, $\%\Pi_{req}$, AND $\%\Pi_{net}$ CORRESPOND TO $t = 1000$. FOR SMALL INITIAL ENERGY, THE PRODUCED AND NET POWERS ARE COMPUTED WITH RESPECT TO LAMINAR UNCONTROLLED FLOW; FOR MODERATE INITIAL ENERGY, THEY ARE COMPUTED WITH RESPECT TO TURBULENT UNCONTROLLED FLOW.

from Fig. 2(a), the energy of the uncontrolled flow exhibits a transient growth followed by an exponential decay to zero. We see that a DTW moves the transient response peak to a smaller time, which is about half the time at which peak of $E(t)$ in the flow with no control takes place. Furthermore, maximal transient growth of the uncontrolled flow is reduced by approximately 2.5 times, and a much faster disappearance of the velocity fluctuations is achieved. On the other hand, Fig. 2(b) clearly exhibits the negative influence of the UTWs on a transient response. In particular, the two UTWs with larger amplitudes (as selected in [2]) significantly increase the energy of velocity fluctuations. We note that the fluctuations' kinetic energy in a flow subject to a UTW with an amplitude as small as $\alpha = 0.015$ at $t = 1000$ is already about two orders of magnitude larger than the maximal transient growth of the uncontrolled flow.

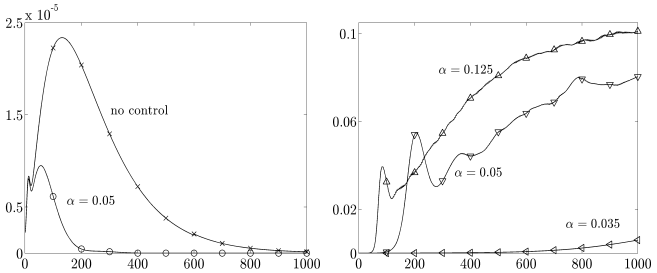

(a) DOWNSTREAM (b) UPSTREAM

Fig. 2. Energy of the velocity fluctuations, $E(t)$, for the initial condition with small energy: (a) $\times$, uncontrolled; $\circ$, a DTW with ($c = 5$, $\omega_x = 2$, $\alpha = 0.05$); and (b) UTWs with $\triangleleft$, ($c = -2$, $\omega_x = 0.5$, $\alpha = 0.015$); $\triangledown$, ($c = -2$, $\omega_x = 0.5$, $\alpha = 0.05$); $\triangle$, ($c = -2$, $\omega_x = 0.5$, $\alpha = 0.125$).

Fig. 3(a) shows the skin-friction drag coefficient as a function of time for the traveling waves considered in Fig. 2. The skin-friction drag coefficient is defined as [9]

$$C_f(t) \;=\; \frac{2\overline{\tau}_w}{U_B^2} \;=\; \frac{1}{R_c\, U_B^2}\left[\left(\frac{\mathrm{d}\overline{U}}{\mathrm{d}y} + \frac{\mathrm{d}\overline{u}}{\mathrm{d}y}\right)\bigg|_{y=-1} - \left(\frac{\mathrm{d}\overline{U}}{\mathrm{d}y} + \frac{\mathrm{d}\overline{u}}{\mathrm{d}y}\right)\bigg|_{y=1}\right], \tag{3}$$

where $\overline{\tau}_w$ denotes the nondimensional average wall-shear stress and

$$U_B(t) \;=\; \frac{1}{2}\int_{-1}^{1} \left(\overline{U}(y) + \overline{u}(y,t)\right)\, \mathrm{d}y,$$

is the total bulk flux. Since both the uncontrolled flow and the flow subject to a DTW stay laminar, their drag coefficients at the steady-state agree with the nominal values computed in the absence of velocity fluctuations (cf. Tables I and II). On the other hand, the drag coefficients of the UTWs that become turbulent are about twice the values predicted using the base flow analysis. The large growth of velocity fluctuations by UTWs has dramatically reduced the nominal flux and consequently increased the drag coefficients. The velocity fluctuations in the UTW with $\alpha = 0.015$ are not amplified enough to have a pronounced effect on the drag coefficient. Furthermore, the drag coefficients for the UTWs with ($c = -2$, $\omega_x = 0.5$, $\alpha = \{0.05, 0.125\}$) at $t = 1000$ agree with the results of [2] computed for the fully developed channel flow. This indicates that the UTWs with larger amplitudes in our simulations have transitioned to turbulence. The above results confirm the theoretical prediction of [1] where it is shown that the UTWs are poor candidates for transition control for they enhance growth of the velocity fluctuations relative to the uncontrolled flow.

The net power as a function of time for the initial conditions with small kinetic energy are shown in Fig. 3. Note that the normalized net power for all traveling waves is negative

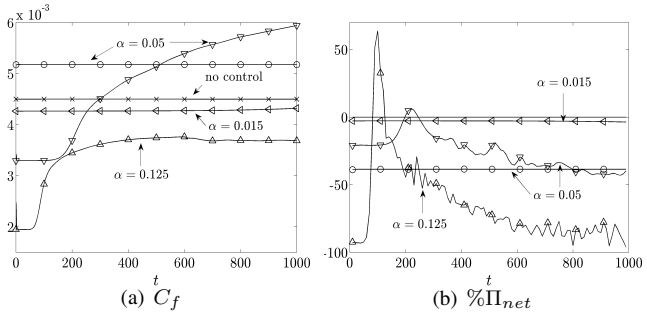

(a) C_f (b) $\%\Pi_{net}$

Fig. 3. (a) Friction drag-coefficient, C_f and (b) normalized net power, $\%\Pi_{net}$, for the initial condition with small energy: $\times$, uncontrolled; $\circ$, DTW with $(c = 5,\ \omega_x = 2,\ \alpha = 0.05)$; and UTWs with $\triangleleft$, $(c = -2,\ \omega_x = 0.5,\ \alpha = 0.015)$; $\triangledown$, $(c = -2,\ \omega_x = 0.5,\ \alpha = 0.05)$; $\triangle$, $(c = -2,\ \omega_x = 0.5,\ \alpha = 0.125)$.

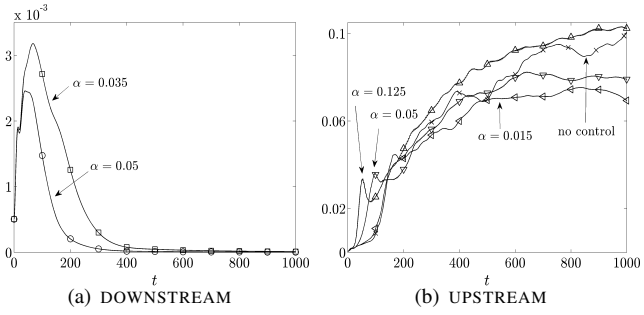

(a) DOWNSTREAM (b) UPSTREAM

Fig. 4. Energy of the velocity fluctuations, $E(t)$, for the initial condition with moderate energy: (a) DTWs with $\square$, $(c = 5, \omega_x = 2, \alpha = 0.035)$; $\circ$, $(c = 5, \omega_x = 2, \alpha = 0.05)$; and (b) $\times$, uncontrolled flow; and UTWs with $\triangleleft$, $(c = -2, \omega_x = 0.5, \alpha = 0.015)$; $\triangledown$, $(c = -2, \omega_x = 0.5, \alpha = 0.05)$; $\triangle$, $(c = -2, \omega_x = 0.5, \alpha = 0.125)$.

(cf. Fig. 3(b)). This agrees with a recent study of [10] where it was established that the net cost to drive a flow by any transpiration-based strategy is larger than in the uncontrolled laminar flow. Furthermore, the above results confirm the prediction of [1] that the net power is negative whenever the uncontrolled flow stays laminar. It is noteworthy that the UTW with $\alpha = 0.125$ has a negative net power despite its significantly smaller drag coefficient compared to the laminar uncontrolled flow. As evident from Table II, this is because the required power for maintaining this UTW is much larger than the power produced by reducing drag.

B. Moderate initial energy

We next consider the velocity fluctuations with moderate initial energy, $E(0) = 5.0625 \times 10^{-4}$. This selection illustrates a situation where the initial conditions are large enough to trigger turbulence in the uncontrolled flow but small enough to allow the properly chosen DTWs to maintain the laminar flow and achieve a positive net power balance. As shown in § III-A, the UTWs trigger turbulence even for the initial conditions whose kinetic energy is about 200 times smaller than the value considered here. The energy of the velocity fluctuations as a function of time is shown in Fig. 4. Fig. 4(b) indicates that the kinetic energy of the uncontrolled flow and the flows subject to UTWs is increased by orders of magnitude which eventually results in transition to turbulence. Conversely, Fig. 4(a) shows that the DTWs significantly weaken intensity of the velocity fluctuations which facilitates maintenance of the laminar flow.

As evident from Fig. 5(b), the large fluctuations' energy in both the uncontrolled flow and in UTWs yields much larger drag coefficients compared to the nominal values reported in Table I. In addition, Fig. 5(b) is in agreement with [2] where it was shown that the skin-friction drag coefficients of the UTWs are smaller than in the uncontrolled flow that becomes turbulent, and that the UTW with $(c = -2,\ \omega_x = 0.5,\ \alpha = 0.125)$ achieves a sub-laminar drag. From Fig. 5(a) we also see that, in flows controlled by DTWs, the small transient growth of fluctuations' kinetic energy results in a small transient increase in the drag coefficients which eventually decay to their nominal values reported in Table I.

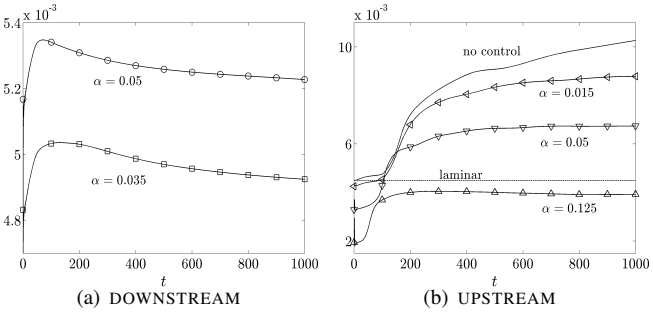

(a) DOWNSTREAM (b) UPSTREAM

Fig. 5. Skin-friction drag coefficient, $C_f(t)$, for the initial condition with moderate energy: (a) DTWs with $\square$, $(c = 5, \omega_x = 2, \alpha = 0.035)$; $\circ$, $(c = 5, \omega_x = 2, \alpha = 0.05)$; and (b) $\times$, uncontrolled flow; and UTWs with $\triangleleft$, $(c = -2, \omega_x = 0.5, \alpha = 0.015)$; $\triangledown$, $(c = -2, \omega_x = 0.5, \alpha = 0.05)$; $\triangle$, $(c = -2, \omega_x = 0.5, \alpha = 0.125)$.

Even though these drag coefficients are larger than in the uncontrolled laminar flow, they are still smaller than in the uncontrolled flow that becomes turbulent (cf. Table II).

The net power for initial condition with moderate kinetic energy are shown in Fig. 6. As can be seen from Table II, the normalized produced power for the DTWs is positive by virtue of the fact that the uncontrolled flow becomes turbulent while the controlled flows stay laminar. Fig. 6(a) shows that the DTW with $\alpha = 0.035$ (respectively, $\alpha = 0.05$) has a positive (respectively, negative) net power balance. The reason for this is twofold: first, the DTW with larger α results in a smaller produced power since it induces a larger negative nominal bulk flux than the DTW with smaller α; and second, the required power to maintain the DTW with larger α is bigger than in the DTW with smaller α. Therefore, we confirm the prediction of [1] that the amplitude of the DTW should be large enough to prevent transition but small enough to yield a positive net power balance. On the other hand, the UTW with $\alpha = 0.015$ is capable of producing a small positive net power for two main reasons: (a) it has a smaller drag coefficient than the uncontrolled turbulent flow (although it becomes turbulent itself); and (b) it requires a much smaller power compared to the UTW with $\alpha = 0.125$. Furthermore, it is noteworthy that at $t = 1000$, the DTW with $\alpha = 0.035$ has a larger net power than the UTW with

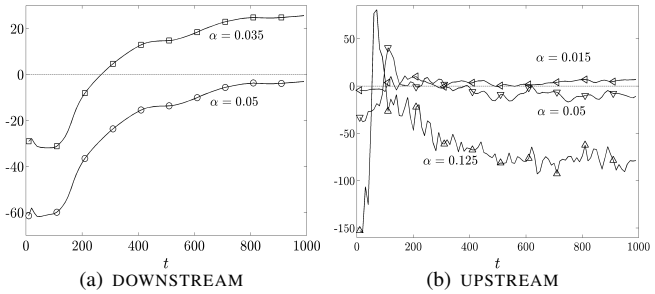

(a) DOWNSTREAM (b) UPSTREAM

Fig. 6. Normalized net power, $\%\Pi_{net}$, in flows subject to (c) DTWs and (d) UTWs, for the initial condition with moderate energy: DTWs with $\square$, $(c = 5, \omega_x = 2, \alpha = 0.035)$; $\circ$, $(c = 5, \omega_x = 2, \alpha = 0.05)$; and UTWs with $\triangleleft$, $(c = -2, \omega_x = 0.5, \alpha = 0.015)$; $\triangledown$, $(c = -2, \omega_x = 0.5, \alpha = 0.05)$; $\triangle$, $(c = -2, \omega_x = 0.5, \alpha = 0.125)$.

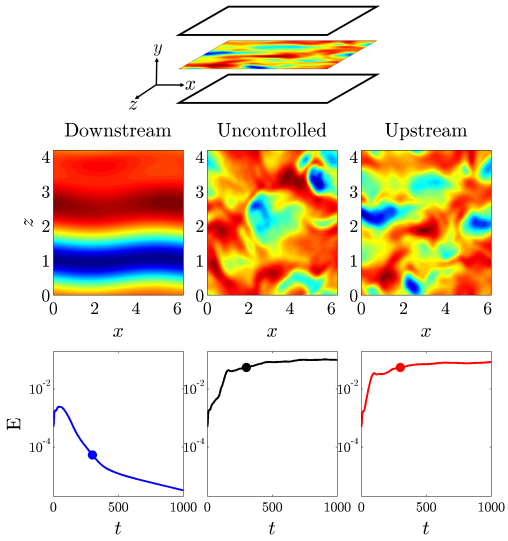

Fig. 7. Color plots: streamwise velocity fluctuations at the center plane of the channel at time $t = 300$ for the uncontrolled flow, flows subject to a DTW with $(c = 5, \omega_x = 2, \alpha = 0.05)$, and a UTW with $(c = -2, \omega_x = 0.5, \alpha = 0.05)$ for the initial condition with moderate energy. Last row: fluctuations' kinetic energy as a function of time.

$\alpha = 0.015$ ($\%\Pi_{net} = 25.63$ vs. $\%\Pi_{net} = 6.83$; cf. Table II). This is because in contrary to the UTW with $\alpha = 0.015$, the DTW with $\alpha = 0.035$ remains laminar and produces a much larger power than it requires.

In the above discussions, transition was identified by examining the fluctuations' kinetic energy and drag coefficient. Large levels of sustained kinetic energy and substantial increase of the drag coefficient (compared to base flow) were used as indicators of transition. Here, we use flow visualization to compare coherent structures in uncontrolled and controlled flows. The onset of transition is characterized by formation of streamwise streaks (structures that are elongated in the x-direction, with a preferential length-scale in the z-direction) and their subsequent break-down. For the initial condition with moderate energy, Fig. 7 shows (i) the color plots of streamwise velocity fluctuations at the channel center plane at $t = 300$; and (ii) the fluctuations' kinetic energy for the uncontrolled flow, a DTW with $(c = 5, \omega_x = 2, \alpha = 0.05)$, and a UTW with $(c = -2, \omega_x = 0.5, \alpha = 0.05)$. As a result of the initial perturbation, streamwise streaks are formed in all three flows (not shown). As evident from Fig. 7, the velocity fluctuations experience significant growth in both the uncontrolled flow and in the flow subject to the UTW; this growth promotes departure from the laminar flow and transition to turbulence. On the contrary, the DTW reduces the growth of fluctuations' energy, thereby weakening intensity of the streaks and maintaining the laminar flow.

IV. Concluding Remarks

This work along with a companion paper [1] represent a continuation of a recent effort [11] to develop a *model-based approach* for design of sensorless flow control strategies in wall-bounded shear flows. Input-output analysis of the linearized NS equations was used as a basis for selection of control parameters for preventing transition to turbulence in [1]. The theoretical predictions provided by this analysis are verified in this paper by direct numerical simulations of the full nonlinear NS equations. This eliminates the need for extensive numerical simulations in the early stages of the design process and facilitates a computationally efficient way of predicting the essential trends.

We show that the DTWs are capable of maintaining the laminar flow and achieving positive net efficiency. This is facilitated by significant reduction of the fluctuations' kinetic energy. In contrast, the UTWs promote turbulence even when the uncontrolled flow remains laminar. We also note that, in spite of promoting turbulence, the UTWs may still achieve smaller drag coefficients compared to the uncontrolled flow. By increasing the UTW amplitude, even sub-laminar drag can be attained (as originally shown in [2]). In flows subject to a fixed pressure gradient, our result show that this comes at the expense of high cost of control (i.e., poor net efficiency).

References

[1] R. Moarref and M. R. Jovanović, "Preventing transition to turbulence using streamwise traveling waves: theoretical analysis," in *Proceedings of the 2010 American Control Conference*, Baltimore, MD, 2010, to appear.

[2] T. Min, S. M. Kang, J. L. Speyer, and J. Kim, "Sustained sub-laminar drag in a fully developed channel flow," *J. Fluid Mech.*, vol. 558, pp. 309–318, 2006.

[3] M. Quadrio and P. Ricco, "Critical assessment of turbulent drag reduction through spanwise wall oscillations," *J. Fluid Mech.*, vol. 521, pp. 251–271, 2004.

[4] J. F. Gibson, "Channelflow: a spectral Navier-Stokes solver in C++," *Tech. Rep.*, 2007, Georgia Institute of Technology, www.channelflow.org.

[5] R. Peyret, *Spectral Methods for Incompressible Viscous Flow*. New York, NY: Springer, 2002.

[6] C. Canuto, M. Y. Hussaini, A. Quarteroni, and T. A. Zang, *Spectral Methods in Fluid Dynamics*. New York, NY: Springer-Verlag, 1988.

[7] J. Hoepffner and K. Fukagata, "Pumping or drag reduction?" *J. Fluid Mech.*, vol. 635, pp. 171–187, 2009.

[8] I. G. Currie, *Fundamental Mechanics of Fluids*. CRC Press, 2003.

[9] W. D. McComb, *The Physics of Fluid Turbulence*. New York: Oxford University Press Inc., 1991.

[10] T. R. Bewley, "A fundamental limit on the balance of power in a transpiration-controlled channel flow," *J. Fluid Mech.*, vol. 632, pp. 443–446, 2009.

[11] M. R. Jovanović, "Turbulence suppression in channel flows by small amplitude transverse wall oscillations," *Phys. Fluids*, vol. 20, no. 1, p. 014101, January 2008.